A Numerical Procedure to Determine the Power Intake/Delivery Capacity of a GaN RF Power Transistor over Broadband

Sedat Kilinc, Malik E. Ejaz, B.S. Yarman, Serdar Ozoguz, Saket Srivastava and Edmond Nurellari

Abstract—**In this paper, a novel "Real Frequency Line Segment Technique" based numerical procedure is introduced to assess the gain-bandwidth limitations of the given source and load impedances, which in turn results in the ultimate RF-power intake/delivering performance of the amplifier. During the numerical performance assessments process, a robust tool called "Virtual Gain Optimization" is presented. Finally, a new definition called "Power-Performance-Product" is introduced to measure the quality of an active device. Examples are presented to assess the gain-bandwidth limitations of the given source and load pull impedances for the 45W-GaN power transistor of Wolfspeed "CG2H40045" over 0.8 -3.8 GHz bandwidth.**

Index Terms—**Positive Real Functions, Foster Functions, Minimum Functions, Real Frequency Techniques, Broadband Matching, Gain-Bandwidth Limitation, Broadband Power Amplifier, GaN Transistor**

I. INTRODUCTION

FOR wireless communication systems, it is essential to design power amplifiers (PA) for variety of applications [1-6]. Nowadays, it is a common practice to employ Gallium Nitrate (GaN) transistors due to their high-power delivering capacity [7-11]. In practice, PA design process starts with careful selection of the power transistor considering the design parameters such as the required output signal power to be delivered, power added efficiency (PAE) of the amplifier, transducer power gain (TPG) over the specified bandwidth etc. Once the power transistor is selected, its nonlinear behavior is characterized by determining the optimum source-pull (SP) and load-pull (LP) impedances.

Let $Z_{SPa}(j\omega_a) = R_{SPa}(\omega_a) + jX_{SPa}(\omega_a)$ and $Z_{LPa}(j\omega_a) = R_{LPa}(\omega_a) + jX_{LPa}(\omega_a)$ designate the discrete actual source and load pull impedance data at the actual angular frequency $\omega_a = 2\pi f_a$ with actual frequency f_a. In these notations, subscript "a" refers to measured actual values. To simplify the PA design process, measured impedance data is normalized with respect to a normalization resistance R_0 and a frequency f_{0a}. In

practice, R_0 may be selected as the standard termination 50Ω and f_{0a} can be chosen at the high end of the frequency band. In this case, normalized frequencies are designated by $f = \frac{f_a}{f_{a0}}$, which is equal to normalized angular frequencies $\omega = \frac{2\pi f_a}{2\pi f_0} = f$. Using the generic notation, a normalized impedance $Z(j\omega)$ is obtained by dividing the actual impedance $Z_a(j\omega_a) = R_a(\omega_a) + jX_a(\omega_a)$ to R_0 such that $Z(j\omega) = \frac{Z_a}{R_0} = R(\omega) + jX(\omega)$. Normalized frequencies are designated by f or equivalently normalized angular frequencies is designated by $\omega = 2\pi f$. Likewise, normalized SP and LP impedances are represented by $Z_{SP}(j\omega) = R_{SP}(\omega) + jX_{SP}(\omega)$ and $Z_{LP}(j\omega) = R_{LP}(\omega) + jX_{LP}(\omega)$ respectively. It is noted that the generated SP and LP terminations optimize the TPG as well as the PAE of the amplifier under consideration. Obviously, source and load impedances must be positive real (PR) functions so that one is able to analytically model the measured data and construct the front and the back-end matching networks as depicted in Fig. 1.

In section II, we propose a novel numerical process to assess the gain-bandwidth limitation of a given impedance data using the "Real Frequency-Line Segment Technique (RF-LST)" [12-15]. During the numerical performance assessments process, we introduce an original tool called "Virtual Gain Optimization (VGO)". In sections III and IV, "Gain-Bandwidth Limitations (GBWL)" of the source pull and the load pull impedances of the Cree CG2H-40045 GaN power transistor is determined over $0.8GHz - 3.8GHz$ bandwidth respectively. In Section V, we introduce a new definition to assess the Power-Intake and Power-Delivery performance of an active device. Finally, the paper is concluded in Section VI.

II. NUMERICAL ASSESSMENT OF THE GAIN-BANDWIDTH LIMITATION OF A REALIZABLE IMMITTANCE

The purpose of this section is to build the best realizable line-segment model for the reported source and load pulled

Sedat Kilinc is with Istanbul University-Cerrahpasa, and he is a Ph.D. student at Istanbul Technical University, Turkey. (e-mail: sedatkilinc@itu.edu.tr).

Malik Ejaz is a Ph.D. student at University of Lincoln, Brayford Pool, Lincoln LN67TS UK (e-mail: mejaz@lincoln.ac.uk).

B.S. Yarman is with Istanbul University-Cerrahpasa, Istanbul Technical University, Turkey and Lincoln University, Lincolnshire, UK, and RFT Research Corporation of Teknopark Istanbul, Turkey. (e-mail: sbyarman@gmail.com).

Serdar Ozoguz is with Istanbul Technical University, Turkey, (e-mail: ozoguz@itu.edu.tr).

Saket Srivastava is with University of Lincoln, Brayford Pool, Lincoln LN67TS UK. (e-mail: ssrivastava@lincoln.ac.uk)

Edmond Nurellari is with University of Lincoln, Brayford Pool, Lincoln LN67TS UK. (e-mail: enurellari@lincoln.ac.uk)
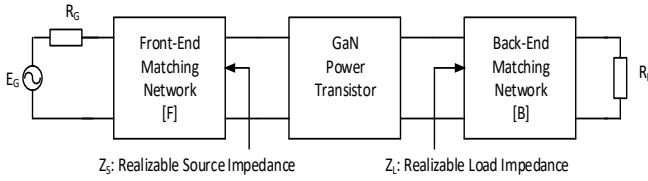
Fig. 1. A typical microwave power amplifier with realizable source and load impedances Z_S and Z_L.

$\kappa_Q(j\omega) = R_Q(\omega) + jX_Q(\omega)$

Fig. 2. A virtual single matching problem to model a measured immittance data $K(j\omega)$ by setting $K_{VL} = Z^*$.

immittances of [16] as much as possible. The proposed method is outlined as follows.

Let $K(j\omega) = R(\omega) + jX(\omega)$ refers to either the optimum source or load pull immittance to be modelled. In this regard, we define a virtual matching problem as shown in Fig. 2, where the virtual load $K_{VL}(j\omega) = R_{LV}(\omega) + jX_{VL}(\omega)$ is the complex conjugate of the immittance data to be modelled using the Real Frequency Line Segment technique [14]. In this case, the virtual load $K_{VL}(j\omega)$ is expressed as

$$R_{LV}(\omega) = R(\omega) \qquad (1a)$$
$$X_{VL} = -X(\omega) \qquad (1b)$$

Referring to Fig.2, in RF-LST, lossless matching network [E], is described by means of its PR driving point back-end immittance $K_Q(j\omega) = R_Q(\omega) + jX_Q(\omega)$ in Darlington sense. Furthermore, we assume that $K_Q(j\omega)$ is a minimum function. Therefore, $X_Q(\omega)$ is uniquely determined from $R_Q(\omega)$ via Hilbert Transformation such that

$$X_m(\omega) = R_\infty + \frac{2\omega}{\pi} \int_0^\infty \frac{R(y)}{y^2 - \omega^2} dy = H\{R(\omega)\} \qquad (2)$$

The real part $R(\omega)$ of a minimum function may be piece-wise linearized as shown in Fig. 3. In Fig. 3, $R(\omega)$ is sampled at the break frequencies $\{\omega_1, \omega_2, \omega_3, ... \omega_N\}$ with corresponding break points $\{R_1, R_2, R_3, ... R_N\}$. Furthermore, it is assumed that adjacent sampled pairs $\{\omega_j, R_j\}$ and $\{\omega_{j+1}, R_{j+1}\}$ are connected by line segments. For a sufficiently large frequency placed at $\omega = \omega_N$, $R(\omega)$ becomes practically zero yielding $R_N = 0$. Based on the line-segment representation of Fig. 3, $R(\omega)$ is simply evaluated using the following line equation. For $\omega_j \leq \omega \leq \omega_{j+1}$ such that $j = 1,2, ..., (N-1)$, $R(\omega)$ is given by

$$R_j(\omega) = a_j\omega + b_j \qquad (3)$$

where $a_j = \frac{R_j - R_{j+1}}{\omega_j - \omega_{j+1}}$ and $b_j = \frac{(R_{j+1})\omega_j - (R_j)\omega_{j+1}}{\omega_j - \omega_{j+1}}$.

In the above representation of $R(\omega)$, we assume that $R_\infty = \lim_{p \to \infty} R(\omega)$ is zero. This is a practical assumption for all passband amplifier designs.

Having line-segment representation of $R(\omega)$, imaginary part $X_m(\omega)$ of (2) is derived as

$$X_m(\omega) = \sum_{j=1}^{N-1} \beta_j(\omega)\Delta R_j \triangleq H\{R(\omega)\} \qquad (4a)$$

where ΔR_j and $\beta_j(\omega)$ is given by

$$\Delta R_j = R_{j+1} - R_j \qquad (4b)$$
$$F_j(\omega) = (\omega + \omega_j) \ln(|\omega + \omega_j|) + (\omega - \omega_j) \ln(|\omega - \omega_j|) \qquad (4c)$$
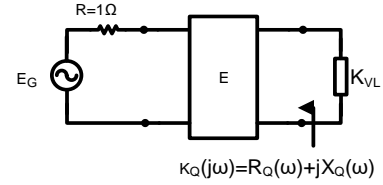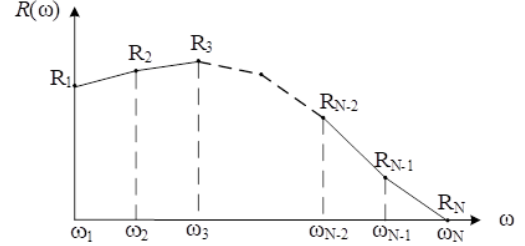

Fig. 3. Piecewise linearization of the Real part $R(\omega)$ of a minimum function $K_m(j\omega) = R(\omega) + jX_m(\omega)$.

$$\beta_j(\omega) = \frac{1}{\pi(\omega_j - \omega_{j+1})} [F_{j+1}(\omega) - F_j(\omega)] \qquad (4d)$$

It is noted that (3) and (4) are easily programmed in MatLab. Thus, one can generate a minimum function $K_m(j\omega)$ point by point from its real part $R(\omega)$ as it is specified in the form of line-segments without using any analytic forms. Resulting $K_m(j\omega) = R(\omega) + jX_m(\omega)$ is for sure positive real.

Referring to Fig. 2, the unknown of the matching problem is selected as the real part $R_Q(\omega)$ and it is expressed by means of its unknown break points $RQA = [R_1 \, R_2 \, R_3 \, ... R_{N-1} \, R_N]$, which is sampled at the break frequencies $WBR = [\omega_1 \, \omega_2 \, \omega_3 \, ... \, \omega_{N-1} \, \omega_N]$. $R_Q(\omega)$ is evaluated using (3) and $X_Q(\omega)$ is generated employing (4).

The unknown break points $[R_1 \, R_2 \, R_3 \, ... R_{N-1} \, R_N]$ are determined to optimize the transducer power gain which is given by

$$T(\omega) = \frac{4R_Q R_{LV}}{(R_Q + R_{LV})^2 + (X_Q + X_{LV})^2}$$
$$= \frac{4R_Q R}{[R_Q + R]^2 + [H(R_Q) - X]^2} \qquad (5)$$

During the optimization process, we target a flat gain level T_0 to minimize the error function $\varepsilon(\omega) = T(\omega) - T_0$ over the frequency band of interest. The ideal solution is the unity TPG (i.e., $T(\omega) = 1$) over passband, which yields $R_Q(\omega) = R(\omega)$ and $X_Q(\omega) = -X_{LV} = X(\omega)$ as desired. As $T(\omega)$ deviates from unity gain, the trace of line segment model shifts from the original data. Therefore, we say that "quality of immittance modelling" is measured by means of the transducer power gain of the virtual matching problem over the passband. During optimization, the error function may be expressed in terms of the unknown break points as

$$\varepsilon(\omega) = T(\omega) - T_0$$
$$= \frac{4R_Q R}{[R_Q(\omega) + R(\omega)]^2 + [\sum_{j=1}^{N-1} \beta_j(\omega)\Delta R_j - X(\omega)]^2} - T_0 \qquad (6a)$$

or equivalently,

$$\varepsilon(\omega) = 4R_Q R - T_0 \left\{ \left[R_Q(\omega) + R(\omega) \right]^2 \right.$$
$$\left. + \left[\sum_{j=1}^{N-1} \beta_j(\omega) \Delta R_j) - X(\omega) \right]^2 \right\} \qquad (6b)$$

In (6), $R(\omega)$ and $X(\omega)$ are the augmented immittance data to be modelled. $R_Q(\omega)$ is a line between the endpoints (ω_j, R_j) and (ω_{j+1}, R_{j+1}) for $\omega \in [\omega_j, \omega_{j+1}]$ as in (3).

It must be noted that $\varepsilon(\omega)$ is a quadratic/convex function in the unknown break points R_j. Therefore, the numerical minimization process is always convergent, and it is possible to hit global minimum of ε yielding the **"best solution for the break points with the highest value of the minimum of the passband gain"**. Based on the last statement, the following sub-section is presented to assess the numerical gain bandwidth limitation of the given immittance data.

A. The Best Transducer Power Gain T(ω)

Referring to Fig. 2, let $K(j\omega) = R(\omega) + jX(\omega)$ be the given immittance to be modelled as a realizable PR network function using the real frequency-line segment technique (RF-LST). Let $K_Q(j\omega) = R_Q(\omega) + jX_Q(\omega)$ be the RF-LST based minimum Driving Point Input Immittance (DPI) in Darlington sense. Let $T(\omega)$ be the transducer power gain (TPG) of the virtually matched system as specified by (5), which is optimized over the specified normalized angular frequency bandwidth B such that $B = [\omega_{c2} - \omega_{c1}]$.

Let T_{min} be the minimum of $T(\omega)$ in B. Let T_{max} be the maximum of $T(\omega)$ in B. Let $T_{mean} = \frac{T_{max} + T_{min}}{2}$ be the mean value of $T(\omega)$ in B and let $\Delta T = T_{max} - T_{mean} = T_{mean} - T_{min}$ be the gain fluctuation in B.

By trial and error, one can determine a flat gain level T_0 in such a way that T_{min} reaches to its maximum value in B. **This state of TPG is called the "RF-LST based Gain Bandwidth-Limitation, or in short "RFLST-GBWL" of the given complex immittance $K(j\omega)$ over the specified bandwidth B.** In this state, the mean value of the transducer power gain describes the average value of the power transfer with optimum fluctuations. In this state, TPG may be expressed as $T(\omega) = T_{mean} \mp \Delta T$.

During the minimization process of (6), T_0 may be swept starting from the flat gain level $T_0(1) = 0.60$ upto to $T_0(n_k) = 1.00$ with small step sizes δT. For example, δT may be selected as $\delta T = 0.05$. In this case, we define an index k in a loop to minimize the error function $\varepsilon(\omega, T_0(k))$ of (9) for a total number $n_k + 1 = 9$ times. Then, at each step k, we store $K_Q(j\omega, k) = R_Q(\omega, k) + jX_Q(\omega, k)$, $T_{min}(k)$, $T_{max}(k)$, $T_{mean}(k), \Delta T(k)\ T(\omega, k)$ and $T_0(k)$ to determine the optimum "$gain - state$" yielding the "$RFLST\ based\ GBWL$" of the complex termination $K(j\omega) = R(\omega) + jX(\omega)$ over B, which in turn results in the best realizable-DPI in the form of line segments or equivalently as sampled data points.

For all the nonlinear optimization problems, initialization of the knowns is always crucial. Therefore, in the next subsection

we present initialization of the unknown break points R_j for the minimization of the error function $\varepsilon(\omega, T_0(k))$ for a fixed T_0.

B. Initialization of the Nonlinear Minimization Process

Before we introduce the optimization process, for a selected flat gain level T_0 and normalized break frequencies $\{\omega_1, \omega_2, \omega_3, ... \omega_N\}$, the unknown break points $\{R_1,\ R_2,\ R_3, ... R_N\}$ must be initialized. To maximize $T(\omega)$ of (5), the reactance term $(X_Q - X)$ is set to zero to derive the initials break points R_{int-j} such that

$$T_0 \approx \frac{4R_Q R}{[R_Q + R]^2} \qquad (7a)$$

or

$$R_{int-j} = R(\omega_j) \left[\frac{2 - T_0 + 2\mu\sqrt{1 - T_0}}{T_0} \right] \geq 0 \qquad (7b)$$

In (7b), μ is a unimodular constant. It is set to $\mu = +1$ for the high values of initials R_{intH-j} or it is selected as $\mu = -1$ for the low initials R_{intL-j}.

C. Minimization of the error function: $\varepsilon(\omega, R_1, R_2, ..., R_{N-1})$

We use MatLab's nonlinear equation solver which is called "$lsqnonlin$" to minimize the sum of square errors ϵ such that

$$\epsilon = \sum_{r=1}^{Ns} [\varepsilon(\omega_r, R_1, R_2, R_3, ..., R_{N-1})]^2; \omega_{c1} \leq \omega_r \leq \omega_{c2} \qquad (8)$$

In (8), the integer Ns is the total number of sampling points over the passband $B = [\omega_{c2} - \omega_{c1}]$ subject to optimization. The normalized angular frequencies ω_{c1} is the low-end and ω_{c2} is the high-end of the frequency band. Thus, the unknown break points $x = \{R_1, R_2, R_3, ..., R_{N-1}\}$ are determined to minimize the sum of squares error ϵ. Minimization is performed using the Levenberg-Marquardt algorithm [17-19].

During minimization of sum of squares error, the first break point R_1 may be kept constant as it is initialized. This constant value may be zero for bandpass problems (i.e., $R_1 = 0$) or it may be included among the unknown break points. At the end of the minimization process, the realizable-driving point input immittance $K_Q(j\omega) = R_Q(\omega) + jX_Q(\omega)$ is obtained which is the optimum possible line-segment model for the measured immittance data $K(j\omega) = R(\omega) + jX(\omega)$.

Thus, we propose the following algorithm to assess the GBWL of the given immittance data. In the algorithm, the virtual matching problem of Fig. 2 is considered, and its virtual gain is optimized. This process is called the "Virtual Gain Optimization" or in short "VGO".

At this point, it is important to re-emphasize that the error function of (6b) is a convex function of the unknown break points R_i, regardless it's total numbers. Therefore, Algorithm always hits the global minimum of the error function, which in turn yields the best solution for the selected flat gain level T_0 over the specified bandwidth. Thus, we say that **RF-LST never requires to select a circuit topology nor an analytic form of a transfer function to optimize the transducer power gain of the matched structure under consideration. Hence, the ultimate gain-bandwidth limitation of the given source and load pull impedances are automatically determined.**
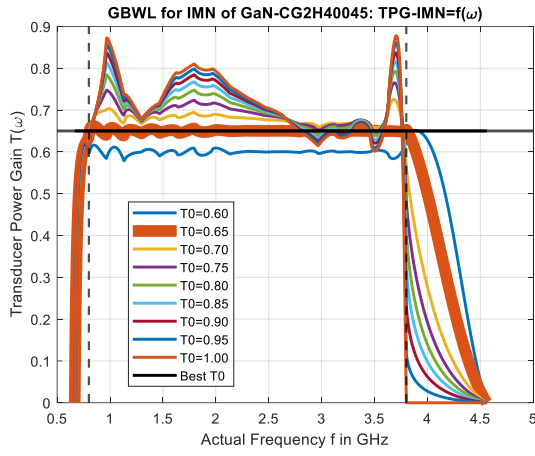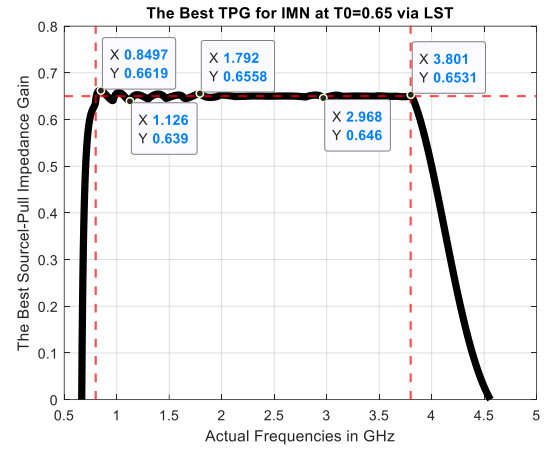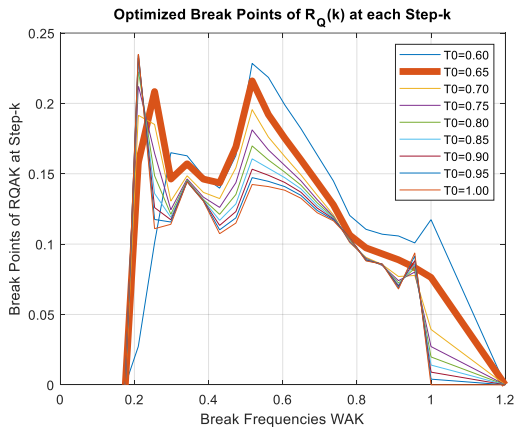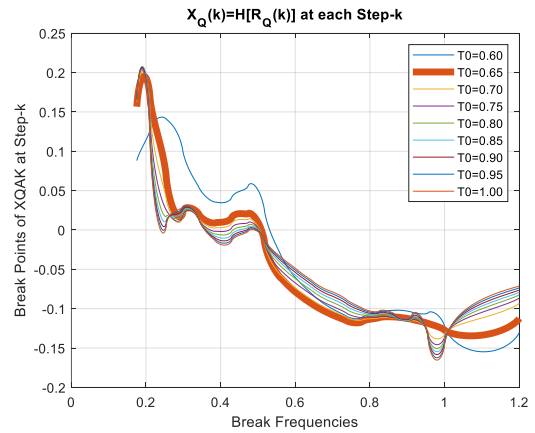
(a) GBWL by sweeping $T_0(k)$ obtained for the source pull data.

Fig. 4. GBWL for the optimum source pull data.

(b) The best TPG obtained for $T0 = 0.65$.

(a) Optimized $R_{QA}(\omega)$.

Fig. 5. Optimized minimum $Z_{QA}(j\omega) = R_{QA}(\omega) + jX_{QA}(\omega)$.

(b) $X_{QA}(\omega) = H\{R_{QA}(\omega)\}$.

Eventually, optimum-realizable source/load pull impedances are obtained as the output of the Algorithm.

III. GAIN BANDWIDTH LIMITATION OF THE SOURCE-PULL IMPEDANCE FOR CREE CG2H40045 GaN TRANSISTOR

In this section, we will investigate the "power-intake" capability of the $Wolfspeed/Cree\_CGH240045$ GaN transistor at its input with the given source-pull data in [16]. Transistor is driven by a generator with $R_0 = 50\ Ohm$ internal resistance. In this regard, it is desired to determine the gain-bandwidth limitation of the given source-pull impedance as detailed in the previous section. User defined passband is specified over $f_{C1} = 800MHz$ and $f_{c2} = 3.8\ GHz$. In this case, we select the normalizing frequency F_0 at $F_0 = 3.8\ GHz$. The real part of the given source-pull impedance is augmented at DC (i.e., $f = 0$) as $RSA(1) = 5\Omega$ and $RSA(N) = 0\Omega$. Similarly, the given imaginary part XSA is augmented as $XSA(1) = 0$ at DC $(i.e. ws1 = 0)$ and the end point is augmented at 6 GHz as $XSA(N) = -25\Omega$. The GBWL of the virtual matching problem is numerically assessed via employing RF-LST algorithm programmed in MatLab.

Results of the sequential optimization of TPG are depicted as in Fig. 4. The RF-LST based Gain Bandwidth Limitation appears to be at $\max(T_{min}) = 0.6390$ with $r = 2$, or equivalently, $T_{mean} = 0.6507 \mp 0.0117$. Optimized break

points $R_{QLST-SP}$ and its corresponding Hilbert Transform $X_{QLST-SP}$ is depicted in Fig. 5a and 5b respectively.

Referring to Fig. 4, it is predicted that 65.07% of the available power of the generator is transferable to the input of the power transistor $CG2H40045$. In other words, GBWL of the optimum realizable source pull impedance is $T_{mean} = 0.6507$ with optimum fluctuation of $\Delta T = \mp 0.0117$.

IV. GAIN BANDWIDTH LIMITATION OF THE LOAD-PULL IMPEDANCE FOR CREE CG2H40045 GaN TRANSISTOR

In this section, we will investigate the power delivering capability of the $Wolfspeed/Cree\_CG2H40045$ GaN transistor at its output-port using the optimum load-pull impedances given in [16]. As in the source-pull gain bandwidth limitation computations, user defined passband is specified over $f_{C1} = 800\ MHz$ and $f_{c2} = 3.8\ GHz$. Therefore, we again set $F_0 = 3.8\ GHz$. The real part of the measured load-pull impedance is augmented at DC (i.e., $f = 0$) as $RLPA(1) = 20\Omega$ and $RLPA(N) = 0\Omega$. Similarly, the measured imaginary part $XLPA$ is augmented as $XLPA(1) = 0$ at DC $(i.e. ws1 = 0)$ and the end point is augmented at 6 GHz as $XLPA(N) = -20\Omega$. The GBWL of the virtual matching problem is numerically assessed via RF-LST employing our MatLab program.

The RF-LST based Gain Bandwidth Limitation appears to be at $\max(T_{min}) = 0.9328$ or equivalently, $T_{mean} = 0.9478 \mp$
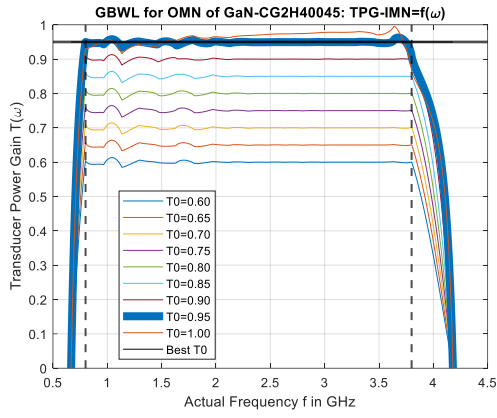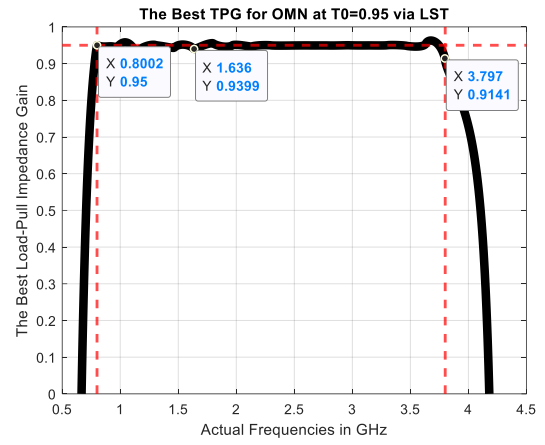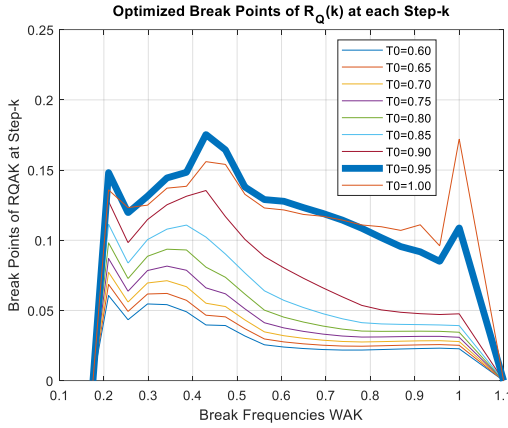
(a) GBWL of LP by sweeping $T0(k)$.

(b) The best TPG obtained for $T0 = 0.95$.

Fig. 6. GBWL for the optimum load pull data.

(a) Optimized $R_{QA}(\omega)$.

(b) $X_{QA}(\omega) = H\{R_{QA}(\omega)\}$.

Fig. 7. Optimized minimum $Z_{QA}(j\omega) = R_{QA}(\omega) + jX_{QA}(\omega)$.

0.015 with corresponding loop index r=8.

The results of sequential optimization of TPG is depicted in Fig. 6. Optimized break points $R_{QLST-LP}$ and its corresponding Hilbert Transform $X_{QLST-LP}$ is depicted in Fig. 7a and 7b respectively.

Referring Fig. 6, it is predicted that 94.78% of the output power is delivered to the load pull impedance of the power transistor $CG2H40045$. In other words, GBWL of the optimum realizable load pull impedance is $T_{mean} = 0.9478$ with optimum fluctuation of $\Delta T = \mp 0.015$.

## V. POWER PERFORMANCE PRODUCT OF AN ACTIVE DEVICE

Considering the results of Section III and Section IV, we can define a new quantity called "Average Power Performance Product $(PPP)_{mean}$" of a power transistor such that

$$(PPP)_{mean} = [GBWL]_{SP} \times [GBWL]_{LP} \quad (9a)$$

where $[GBWL]_{SP}$ is the gain bandwidth limitation of the measured source-pull impedance and $[GBWL]_{LP}$ is the gain bandwidth limitation of the measured load-pull impedance respectively. Thus, we can say that maximum power performance product $(PPP)_{max}$ of an active device cannot exceed

$$(PPP)_{max} = [T_{max}]_{SP} \times [T_{max}]_{LP} \quad (9b)$$

where $[T_{max}]_{SP}$ and $[T_{max}]_{LP}$ the values of the maximum pass band gains which corresponds to $[GBWL]_{SP}$ and $[GBWL]_{LP}$
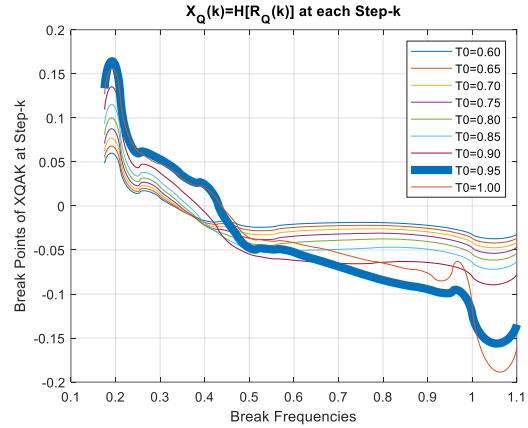
respectively.

By Fig. 4. and Fig 6., for Cree CG2H40045, $(PPP)_{mean} = 0.6507 \times 0.9478 = 0.6167$ (i.e., ~61.7%) and $(PPP)_{max} = 0.6624 \times 0.9628 = 0.6378 = 63.8\%$.

VI. CONCLUSION

An RF power amplifier design process starts with the characterization of the selected active device. The active device may be a GaN power transistor. In this regard, the source/load pull impedances of the active device are generated to optimize the power added efficiency (PAE) as well as the transducer power gain (TPG) of the amplifier over the frequency band of interest. Eventually, based on generated source/load pull impedances the input and the output matching networks of the power amplifier is designed. At this point, it is crucial to note that for many practical situations, source and load pull impedances placed on the Smith Chart, do not necessarily belong to realizable positive functions (PR) over the entire frequency band. In this case, one must check if these impedances are realizable. If not, it is well known that power intake and power delivery performance of the active device may be penalized heavily. In this regard, the designer must evaluate the power transistor properly to decide whether it is worth using it or not. Therefore, in this paper we introduced a new numerical method to assess the "Gain-Bandwidth Limitations (GBWL)"

of the given source and load pull impedances employing the real frequency line segment technique. In this context, gain bandwidth limitations of the given source and load pull impedances yield the power-intake and the power delivery capacity of the selected active device respectively. The proposed numerical assessment method utilizes our newly developed robust "virtual gain optimization" tool called VGO. VGO minimizes a convex error function by targeting its global minimum, which in turn yields the optimum-realizable source and load terminations of the nonlinear active device under consideration. Thus, ultimate power intake and power delivery capacity of the nonlinear active device is determined. Finally, a new definition is introduced to measure the power-intake and power delivery quality of an active device, so called "Power-Performance-Product (in short PPP or 3P) based on the (GBWL) of the given source/load pull impedances.

Employing Cree's CG2H40045 GaN transistor, we exhibit the design of an "optimum performance power amplifier algorithm" using the real frequency line segment technique over $0.8\text{GHz} - 3.8\text{GHz}$ bandwidth which ideally receives average of 65.07% of the available power of the resistive input excitation and delivers the 94.78% of the transistor's output power to a resistive load.

REFERENCES

[1] Li, Meng; Pang, Jingzhou; Li, Yue; Zhu, Anding, "Ultra-Wideband Dual-Mode Doherty Power Amplifier Using Reciprocal Gate Bias for 5G," *IEEE Transactions on Microwave Theory and Techniques,* vol. 10, no. 67, pp. 4246-4259, 14 August 2019.

[2] Yuji Komatsuzaki; Rui Ma; Shuichi Sakata; Keigo Nakatani; Shintaro Shinjo, "A Dual-Mode Bias Circuit Enabled GaN Doherty Amplifier Operating in 0.85-2.05GHz and 2.4-4.2GHz," in *2020 IEEE/MTT-S International Microwave Symposium*, LosAngeles (LA), USA, 2020.

[3] G. Formicone, J. Burger, J. Custer, R. Keshishian and W. Veitschegger, "A Study for Achieving High Power and Efficiency based on High Bias Operation in C- and X-band GaN Power Amplifiers," in *IEEE Topical Conference on Power Amplifiers for Wireless and Radio Applications (PAWR)*, San Diego, CA, USA, 2018.

[4] A. Grebennikov, Radio Frequency and Microwave Power Amplifiers. Volume 1: Principles, Device Modeling and Matching Networks, Institution of Engineering and Technology, 2019.

[5] B. Liu, C. C. Boon, M. Mao, P. Choi and T. Guo, "A 2.4–6 GHz Broadband GaN Power Amplifier for 802.11ax Application," *IEEE Transactions on Circuits and Systems I: Regular Papers,* vol. 68, no. 6, pp. 2404-2417, 2021.

[6] K. Krishnamurthy, T. Driver, R. Vetury, J. Martin, "100 W GaN HEMT Power Amplifier Module with 60% Efficiency over 100-1000 MHz Bandwidth," in *IEEE IMS*, Anaheim, California, USA, 2010.

[7] T. Kikkawa, K. Joshin and M. Kanamura, "GaN Device for Highly Efficient Power Amplifiers," *Fujitsu Sci. Tech. J.,* vol. 48, no. 1, pp. 40-46, 2012.

[8] S. Mizuno, F. Yamada, H. Yamamoto, M. Nishihara, T. Yamamoto and S. Sano, "Development of GaN HEMT for Microwave Wireless Communications," *SEI TECHNICAL REVIEW,* no. 74, pp. 71-74, 2012.

[9] T. Maier, V. Carrubba, R. Quay, F. v. Raay and O. Ambacher, "Active harmonic source-/load-pull measurements of AlGaN/GaN HEMTs at X-band frequencies," in *83rd ARFTG Microwave Measurement Conference*, Tampa, FL, USA, 2014.

[10] K. Inoue, S. Sano, Y. Tateno, F. Yamaki, K. Ebihara, N. Ui, A. Kawano and H. Deguchi, "Development of Gallium Nitride High Electron Mobility Transistor for Cellular Base Stations," *SEI TECHNICAL REVIEW,* no. 71, pp. 88-93, 2010.

[11] R. S. Pengelly, S. M. Wood, J. W. Milligan, S. T. Sheppard and W. L. Pribble, "A Review of GaN on SiC High Electron-Mobility Power Transistors and MMICs," *IEEE Transactions on Microwave Theory and Techniques,* vol. 60, no. 6, pp. 1764-1783, 2012.

[12] H. Carlin, "New approach to gain bandwidth problems," *IEEE Trans. on CAS,* vol. 24, no. 4, pp. 170-175, 1977.

[13] B. S. Yarman, "Chapter 1: Circuit Theory for Power Transfer networks, Section 1.18 Positive Real Functions," in *Design of Ultra Wideband Power Transfer Networks*, West Sussex, UK, Jhon Wiley & Sons Ltd., 2010, pp. 25-33.

[14] B. S. Yarman, "Chapter 11: Modern Approaches to Broadband Matching Problems; Real Frequency Solutions," in *Design of Ultra Wideband Power Transfer Networks*, West Sussex, UK, Jogn Wiley & Sons Ltd, 2010, pp. 539-586.

[15] H. J. Carlin and P. P. Civalleri, in *Wideband Circuit Design,*, New York, CRC Press, 1998.

[16] Wolfspeed a Cree Company, "GaN HEMT Transistor series," https://www.wolfspeed.com/cg2h40045, Durham, North Carolina, USA 27703, 2022.

[17] K. Levenberg, ""A Method for the Solution of Certain Problems in Least-Squares"," p. pp. 164–168, 1944.

[18] D. Marquardt, " "An Algorithm for Least-squares Estimation of Nonlinear Parameters"," *Journal Applied Mathematics,* vol. 11, p. 431–441, 1963.

[19] T. F. Coleman and Y. Li, ""An Interior, Trust Region Approach for Nonlinear Minimization Subject to Bounds"," vol. 6, pp. 418-445, 1996.